

MICROCOPY RESOLUTION TEST CHART
NATIONAL BUREAU OF STANDARDS 1963-A

AD-A153 503

MRC Technical Summary Report #2790

SINGULARITY SOLUTIONS FOR ELLIPSOIDS
IN LOW-REYNOLDS-NUMBER FLOWS: WITH
APPLICATIONS TO THE CALCULATION OF
HYDRODYNAMIC INTERACTIONS IN
SUSPENSIONS OF ELLIPSOIDS

Sangtae Kim

Mathematics Research Center
University of Wisconsin—Madison
610 Walnut Street
Madison, Wisconsin 53705

February 1985

(Received January 31, 1985)

DTIC FILE COPY

Sponsored by
U. S. Army Research Office
P. O. Box 12211
Research Triangle Park
North Carolina 27709

Approved for public release
Distribution unlimited

National Science Foundation
Washington, DC 20550

DTIC
SELECTED
MAY 9 1985
S D

85

4

- 0

111

UNIVERSITY OF WISCONSIN-MADISON
MATHEMATICS RESEARCH CENTER

SINGULARITY SOLUTIONS FOR ELLIPSOIDS IN LOW-REYNOLDS-NUMBER FLOWS:
WITH APPLICATIONS TO THE CALCULATION OF
HYDRODYNAMIC INTERACTIONS IN SUSPENSIONS OF ELLIPSOIDS

Sangtae Kim*

Technical Summary Report #2790
February 1985

ABSTRACT

The disturbance velocity fields due to translational and rotational motions of an ellipsoid in a uniform stream, constant vorticity and constant rate-of-strain, required in fundamental studies of behavior of suspensions, have been obtained by the singularity method. These solutions extend earlier solutions for prolate spheroids. Although equivalent solutions were obtained by Oberbeck (1876), Edwardes (1892) and Jeffery (1922) by separation of variable in ellipsoidal coordinates, the singularity solutions are far more simple in form. Other significant results obtained by the singularity method include the exposition of the unified structure shared by the three boundary value problems and the construction of new forms of the Faxen laws for ellipsoids through application of the reciprocal theorem. The disturbance solutions and Faxen laws, the basis for Smoluchowski's (1911) method-of-reflections technique, are used to calculate hydrodynamic interactions between two or more arbitrarily oriented ellipsoids. In particular, mobility problems are solved directly to order R^{-5} , where R is the centroid-to-centroid separation between the ellipsoids.

AMS (MOS) Subject Classifications: 76D05, 35Q10

Key Words: Sedimentation, Spheroids, Ellipsoids, Low-Reynolds-Number, Hydrodynamic Interaction.

Work Unit Number 2 - Physical Mathematics

*Department of Chemical Engineering and Mathematics Research Center,
University of Wisconsin-Madison, Madison, WI 53706

Sponsored by the United States Army under Contract No. DAAG29-80-C-0041. Material is based upon work supported by the AMOCO Foundation and by the National Science Foundation under Grant Nos. CPE-8404451 and DMS-8210950, Mod. 1.

A

SIGNIFICANCE AND EXPLANATION

The calculation of hydrodynamic interactions between nonspherical particles is needed for the understanding and control of many natural and manufacturing processes, for instance, those involving sedimentation, colloidal stability or suspension rheology. While single-particle solutions for disks, needles (and in general, ellipsoids) are available, such solutions are not easily generalized to multi-particle problems, necessary for examining particle-particle interactions. New forms are presented here which greatly facilitate this task. A model sedimentation problem involving two ellipsoids of revolution is used to illustrate the general technique. Future work will cover other applications of this technique.

Accession For	
NTIS GRA&I	<input checked="" type="checkbox"/>
DTIC TAB	<input type="checkbox"/>
Unannounced	<input type="checkbox"/>
Justification	
By _____	
Distribution/ _____	
Availability Codes	
Dist	Avail and/or Special
A-1	



The responsibility for the wording and views expressed in this descriptive summary lies with MRC, and not with the author of this report.

NOTATION

<u>A</u>	resistance tensor for spheroids.
a	largest semi-axis of ellipsoid.
b	intermediate semi-axis of ellipsoid.
<u>C</u>	resistance tensor for spheroids.
c	smallest semi-axis of ellipsoid.
<u>d</u>	spheroid orientation vector.
<u>E</u>	rate-of-strain tensor.
e	eccentricity of the generating ellipse.
<u>F</u>	force exerted by the fluid on the particle.
f	density function in singularity distributions.
<u>g</u>	gravitational vector.
<u>H</u>	resistance tensor for spheroids, rank = 3.
<u>I</u>	Oseen-Burgers tensor.
<u>L</u>	vector operator in singularity solution.
<u>M</u>	resistance function for spheroids, rank = 4.
<u>n</u>	unit vector normal to the surface.
p	pressure.
q	density function in singularity distributions.
R	center to center separation between two ellipsoids.
r	radial coordinate from particle center.
<u>S</u>	symmetric part of the stress-dipole (stresslet).
<u>T</u>	torque exerted by the particle on the fluid.
<u>T</u>	anti-symmetric part of the stress-dipole.
<u>U</u>	particle translational velocity.

\underline{v}	fluid velocity.
X	resistance function for spheroids.
x	Cartesian coordinate.
\underline{x}	position vector.
\underline{x}'	point on the fundamental ellipse.
Y	resistance function for spheroids.
y	Cartesian coordinate.
Z	resistance function for spheroids.
z	Cartesian coordinate.

Greek Letters

$\alpha_0, \alpha_0', \alpha_0''$	Constants in Jeffery's (1922) solution.
$\beta_0, \beta_0', \beta_0''$	Constants in Jeffery's (1922) solution.
$\gamma_0, \gamma_0', \gamma_0''$	Constants in Jeffery's (1922) solution.
$\underline{\delta}$	identity tensor.
$\underline{\epsilon}$	alternating tensor.
θ	polar angle for spheroids.
μ	fluid viscosity.
ρ	ellipsoidal coordinate (ρ constant gives ellipsoidal surface).
$\underline{\sigma}$	stress tensor.
χ	ellipsoidal harmonic.
Ω	Dirichlet potential
$\underline{\Omega}$	angular velocity of fluid.
$\underline{\omega}$	particle angular velocity.

Subscripts

- 1, 2 labels for particles.
- E refers to the fundamental ellipse
- i, j, k, ℓ , ... indices used in the Einstein summation convention.
- (n) label for multipoles in the singularity solution.

Superscripts

- (n) label for the n-th reflection.
- ∞ ambient field.

SINGULARITY SOLUTIONS FOR ELLIPSOIDS IN LOW-REYNOLDS-NUMBER FLOWS:
WITH APPLICATIONS TO THE CALCULATION OF
HYDRODYNAMIC INTERACTIONS IN SUSPENSIONS OF ELLIPSOIDS

Sangtae Kim*

1. INTRODUCTION

Suspensions of nonspherical particles exhibit non-Newtonian behavior through the interaction between the flow field and Brownian motion (Giesekus (1962), Brenner (1972), Hinch & Leal (1972)). However, rigorous derivation of the material functions to date have been restricted to the dilute limit, partly because of the lack of information on multi-particle hydrodynamic interactions. Existing information on particle-particle interactions is limited to interactions between prolate spheroids in certain geometries such as large particle-particle separations (Wakiya 1965) or special configurations (Gluckman et. al. 1971; Liao & Krueger 1980). Hydrodynamic interactions between oblate spheroids, despite widespread occurrence, e.g. the disk-shaped kaolinite minerals in clay/water suspensions, have received even less attention.

The first steps towards a method-of-reflections solution of multi-ellipsoid, hydrodynamic-interaction problems are presented here. Our primary goal is the solution of problems where the rigid-body motion of the particles are to be determined, given the external forces, torques and the ambient velocity field. Defined by Batchelor (1976) as mobility problems, these problems appear most frequently in the hydrodynamic interaction terms of the rheological theories mentioned above.

*Department of Chemical Engineering and Mathematics Research Center,
University of Wisconsin-Madison, Madison, WI 53706

Our faith in the method-of-reflections approach is based on the experience with spherical particles where it is known that one can solve the mobility problems accurately with a surprisingly small number of reflections (see for example, Felderhof (1977) and Jeffrey & Onishi (1984)). This conclusion appears to hold as well for prolate spheroids. Kim (1984b) has determined the sedimentation velocities of two arbitrarily oriented spheroids accurate to order R^{-5} where R is the centroid-to-centroid separation, using only two reflections beyond the isolated-particle solution.

The method of reflections used here follows Smoluchowski (1911). Readers who are not familiar with the details of this technique are referred to the discussion in Happel & Brenner (1973). The method is summarized as follows. The disturbance velocity field generated by a test particle (call this particle- α) will modify the velocity field seen by other particles (for example, at particle- β). We call the disturbance velocity generated by β in response to the disturbance from α as the "reflected field at β ". This process can be continued indefinitely, with each reflected fields as the incident field at higher order reflections.

The disturbance velocity field of an isolated particle can be considered a reflection with the ambient velocity field as the incident field. We call this the zero-th reflection. The first reflection generates reflected fields at each particle with the zero-th reflection fields from all other particles as the incident fields. For an M -particle suspension, the N -th reflection generates $M \times (M-1)^N$ reflected fields from $M \times (M-1)^{N-1}$ incident fields.

We shall represent the reflected field by a multipole expansion with the multipole moments related to the incident field by Faxen laws (Rallison 1978, Kim 1983). This approach is direct and simple but its success hinges upon the availability of the Faxen laws for the lower order moments.

Brenner (1964) has shown, using the Lorentz (1907) reciprocal theorem, that Faxen laws can be constructed if one knows the stress distribution in the conjugate velocity problem; i.e. the solution for translating ellipsoids, rotating ellipsoids and ellipsoids in a rate-of-strain field are required for the Faxen laws for the force (Brenner 1964), torque (Brenner 1964) and stresslet (Rallison 1978). Furthermore, if the conjugate solution is expressed in terms of the fundamental solution of the Stokes equation, (also known as the Stokeslet) then as noted by Hinch (1977), Brenner's (1964) procedure reduces to the simple statement that the Faxen law for the moment has the same functional form as the conjugate velocity field. An explicit statement and proof is given in Kim (1985a). Therefore, the bulk of the present work is directed towards finding such singularity solutions for ellipsoids.

The singularity method has been used by Chwang & Wu (1974, 1975) to solve exactly the translational, rotational and rate-of-strain problems for prolate spheroids. These solutions are the conjugates for the Faxen force, torque and stresslet law. In their introduction, they review the history of the singularity method, including the pioneering works of Lorentz (1892), Oseen (1927) and Burgers (1938). Other early applications of the singularity method are the works on slender-body theory by Hancock (1953) and Tuck (1964). Less has been done on "thin-body" theory but recent results are available for thin oblate bodies of revolution, e.g. Barshinger & Geer (1984). As stated by Chwang & Wu (1975), "through these investigations, the relative simplicity and effectiveness of the (singularity) method have gradually become more recognized". However, the primary difficulty is that a priori, one does not know the type of singularities and their distributions. In fact, one

objective of the work of Chwang & Wu (1974, 1975), Chwang (1975) was the accumulation of a class of exact solutions by the singularity method. Section 2 of the present work adds the general ellipsoidal shape to this collection.

The organization of this paper is as follows. In Section 2, the ellipsoidal solutions of Oberbeck (1876) and Jeffery (1922) are re-expressed as singularity solutions, i.e. in terms of the fundamental solution of the Stokes equation. (Edwardes' (1892) work is contained within Jeffery's solution). The form of the singularity solution is surprisingly simple. In addition, the singularity method reveals a unified structure which is not apparent in the traditional expressions in ellipsoidal harmonics. This structure suggests new forms for the velocity representations for nonspherical particles in capillaries and other bounded domains. The special case of oblate and prolate ellipsoids of revolution, including a complete discussion of the resistance tensors, is provided in the appendix. Section 3 is a discussion on new forms of the Faxen laws for the force, torque and stresslet on an ellipsoid with applications to the method of reflections for two ellipsoids. The hydrodynamic interactions between two sedimenting oblate spheroids have been determined and are compared with the results obtained in Kim (1985b) for prolate spheroids.

2. THE SINGULARITY SOLUTION FOR ELLIPSOIDS

In this section, we will derive the singularity solution for an ellipsoid in Stokes flow. We will start by describing the classical boundary value problem followed by a description of the singularity solution. The derivation is outlined in the appendix.

2.1 Description

Consider an ellipsoid with semiaxes of lengths a , b and c , with $a \geq b \geq c$. The ellipsoid surface satisfies:

$$\frac{x^2}{a^2} + \frac{y^2}{b^2} + \frac{z^2}{c^2} = 1. \quad (2.1)$$

The governing equations for the velocity, \underline{v} , and pressure, p , are the Stokes equations for low-Reynolds-number flow,

$$-\nabla p + \mu \nabla^2 \underline{v} = \underline{0}, \quad (2.2)$$

where μ is the viscosity; and the equation of continuity for incompressible flow,

$$\nabla \cdot \underline{v} = 0. \quad (2.3)$$

The boundary conditions are:

1) On the ellipsoid surface, \underline{v} is equal to the particle's rigid-body motion:

$$\underline{v} = \underline{U} + \underline{\omega} \times \underline{x} \quad (2.4)$$

2) As $|\underline{x}| \rightarrow \infty$, \underline{v} approaches the ambient velocity, i.e.,

$$\underline{v} \rightarrow \underline{v}^\infty = \underline{U}^\infty + \underline{\Omega}^\infty \times \underline{x} + \underline{E}^\infty \cdot \underline{x}, \quad (2.5)$$

where \underline{U} and $\underline{\omega}$ are the particle translational and rotational velocities and \underline{h}

$\underline{\Omega}^{\infty}$ and \underline{E} are the uniform stream, ambient rotation and rate-of-strain. From (2.4b), it follows that $\underline{\Omega}^{\infty}$ is one-half of $\nabla \times \underline{v}^{\infty}$, the ambient vorticity.

The solution to this problem can be expressed using a distribution of $\underline{I}(\underline{x}-\underline{x}')/(8\pi\mu)$, the fundamental solution of the Stokes equation. \underline{I} , the Oseen-Burgers tensor given by

$$I_{ij} = \frac{1}{r}\delta_{ij} + \frac{1}{r^3}x_i x_j, \quad \text{with } r = |\underline{x}|, \quad (2.5a)$$

and its pressure field,
$$p_j = \frac{2\mu}{r^3}x_j, \quad (2.5b)$$

satisfy the Stokes equation with point forcing,

$$-\frac{\partial p_j}{\partial x_i} + \mu \nabla^2 I_{ij} = -8\pi\mu \delta_{ij} \delta(\underline{x}), \quad (2.6a)$$

and the continuity equation,
$$\frac{\partial I_{ij}}{\partial x_i} = 0 \quad (2.6b)$$

(see Happel & Brenner (1973) Chapter 2).

It is now claimed that the disturbance velocity field, $\underline{v}-\underline{v}^{\infty}$, can be written as:

$$\underline{v}(\underline{x}) - \underline{v}^{\infty}(\underline{x}) = \sum_{n=1}^{\infty} \underline{L}^{(n)} \cdot \int_E f_{(n)}(x', y') \left\{ 1 + \frac{c^2 q^2}{4n-2} \nabla^2 \right\} \underline{I}(\underline{x}-\underline{x}') / (8\pi\mu) dx' dy', \quad (2.7)$$

with
$$f_{(n)}(x, y) = \frac{(2n-1)}{2\pi a_E b_E} q^{2n-3}, \quad (2.8a-e)$$

$$q(x, y) = \left[1 - \frac{x^2}{a_E^2} - \frac{y^2}{b_E^2} \right]^{1/2},$$

$$a_E = (a^2 - c^2)^{1/2}, \quad b_E = (b^2 - c^2)^{1/2},$$

and
$$\underline{L}^{(n)} = \begin{cases} -\underline{E} & \text{if } n=1, \\ \underline{S} \cdot \nabla + \underline{T} \cdot \nabla & \text{if } n=2. \end{cases}$$

The following is a description of the terms which appears in the solution.

REFERENCES

- Barshinger, R.N. & Geer, J.F. 1984 Stokes flow past a thin oblate body of revolution: axially incident flow uniform flow. SIAM J. Appl. Math. 44, 19-32.
- Batchelor, G.K. & Green, J.T. 1972 The hydrodynamic interaction of two small freely-moving spheres in a linear flow field. J. Fluid Mech. 56, 375-400.
- Batchelor, G.K. 1976 Brownian diffusion of particles with hydrodynamic interaction. J. Fluid Mech. 74, 1-29.
- Brenner, H. 1964 The Stokes resistance of an arbitrary particle IV. Arbitrary fields of flow. Chem. Eng. Sci. 19, 703-727.
- Brenner, H. 1972 Suspension rheology. Progress in heat and mass transfer 5, 89-129. Pergamon Press.
- Burgers, J.M. 1938 On the motion of small particles of elongated form suspended in a viscous liquid. Chap. III of Second report on viscosity and plasticity. Kon. Ned. Akad. Wet., 16, 113-184.
- Chwang, A.T. & Wu, T.Y. 1974 Hydromechanics of low-Reynolds-number flow. Part 1. Rotation of axisymmetric bodies. J. Fluid Mech. 63, 607-622.
- Chwang, A.T. & Wu, T.Y. 1975 Hydromechanics of low-Reynolds-number flow. Part 2. Singularity method for Stokes flows. J. Fluid Mech. 67, 787-815.
- Chwang, A.T. 1975 Hydromechanics of low-Reynolds-number flow. Part 3. Motion of spheroidal particles in quadratic flows. J. Fluid Mech. 72, 17-34.
- Edwardes, D. 1892 Steady motion of a viscous liquid in which an ellipsoid is constrained to rotate about a principal axis. Quart. J. Math. 26, 70-78.
- Felderhof, B.U. 1977 Hydrodynamic interaction between two spheres. Physica 89A, 373-384.
- Giesekus, H. 1962 Elasto-viskose Flüssigkeiten, für die in stationären Schichtströmungen sämtliche Normalspannungskomponenten verschieden grosse sind. Rheol. Acta 2, 50-62.
- Gluckman, M.J., Pfeffer, R. & Weinbaum, S. 1971 A new technique for treating multiparticle slow viscous flow: axisymmetric flow past spheres and spheroids. J. Fluid Mech. 50, 705-740.
- Happel, J. & Brenner, H. 1973 Low Reynolds number hydrodynamics. Sijthoff & Noordhoff.
- Hancock, G.J. 1953 The self-propulsion of microscopic organisms through liquids. Proc. Roy. Soc. A217, 96-121.
- Hess, E.J. 1972 Note on the symmetries of certain material tensors for a particle in Stokes flow. J. Fluid Mech. 54, 423-425.

the orientation trajectories are followed from $\theta=0$ (horizontally oriented oblate spheroids and vertically oriented prolate spheroids) the curves in Figures 2 and 3 fall into two groups, depending on the initial value of R . For both oblate and prolate spheroids, if R (at $\theta=0$) exceeds a critical value, then the particles monotonically drift apart. Their orientations approach asymptotically a limiting value of θ , since at large separations ω goes to zero. However, for initial values of R less than the critical value, the rotational motion is sufficiently large to cause the particles to rotate beyond $\theta=\pi/2$, whereafter, the particles drift back towards each other along trajectories which are mirror images of the outward trajectories. The separatrix which starts at the critical value of R has the asymptote $\theta^\infty = \pi/2$ (horizontal orientation).

At large values of R , the trajectories can be approximated accurately by taking just the leading terms on the right-hand-side of evolution equations (3.12) and (3.13). These approximate equations have exact solutions,

$$\text{oblate spheroids:} \quad \frac{1}{R} - \frac{1}{R_0} = (2/3)(1/Y^A - 1/X^A)(\cos 2\theta - \cos 2\theta_0),$$

$$\text{and prolate spheroids:} \quad \frac{1}{R} - \frac{1}{R_0} = (2/3)(1/X^A - 1/Y^A)(\cos 2\theta - \cos 2\theta_0).$$

The resistance functions X^A and Y^A are defined in the appendix.

The influence of the aspect ratio is seen by comparing Figures 2 and 3 for aspect ratios of 10 and 2 respectively. As the aspect ratio is reduced, the region occupied by periodic trajectories enlargens and the trajectories straighten into the vertical lines of the spherical case. Finally, at a fixed aspect ratio, stronger hydrodynamic interactions between oblate spheroids result in a far greater region of periodic trajectories.

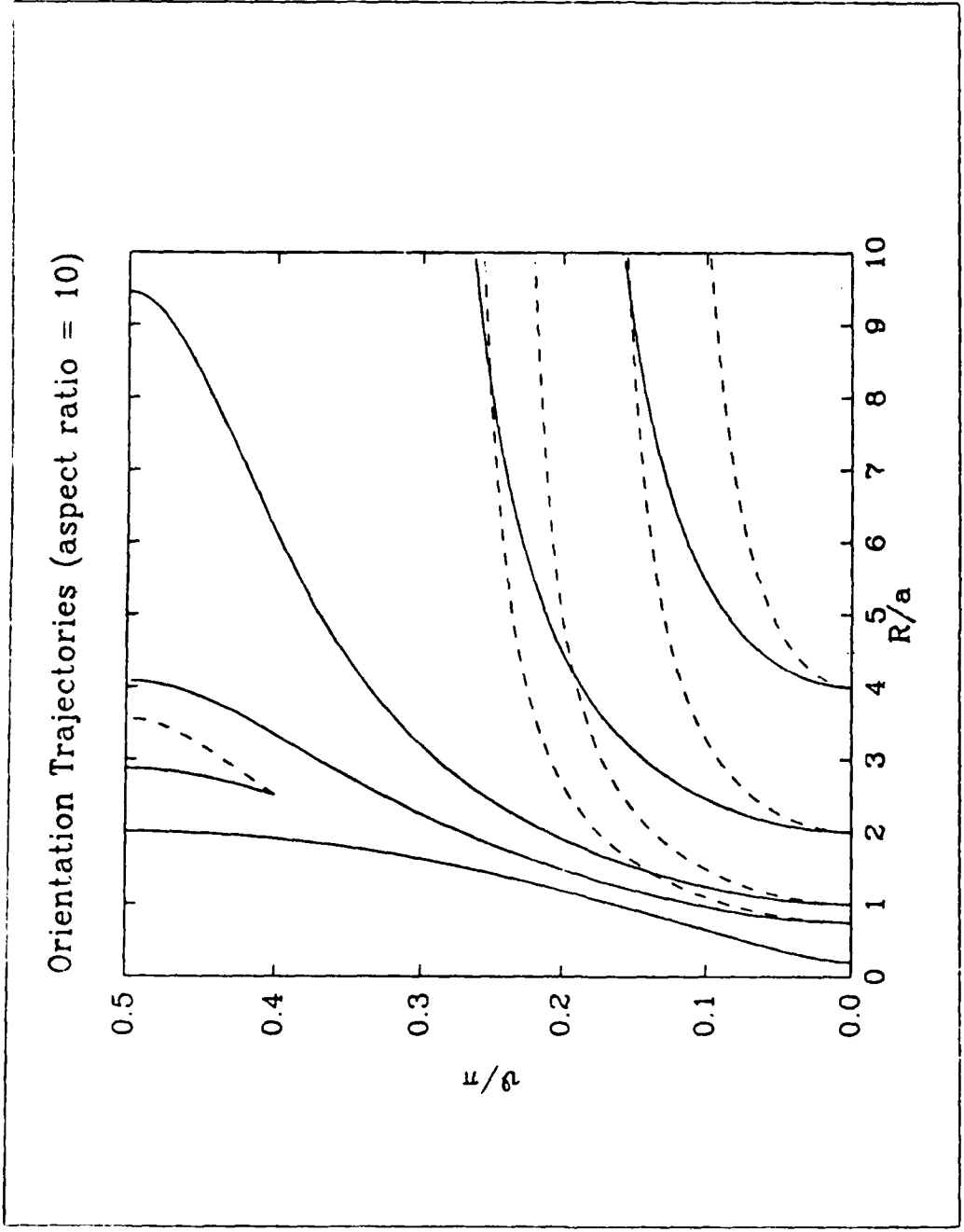


Figure 3. Evolution of orientation and separation between two spheroids, aspect ratio = 2, settling as in Figure 1. The solid and dashed trajectories are for oblate and prolate spheroids respectively. The separatrix goes through the x on the right border.

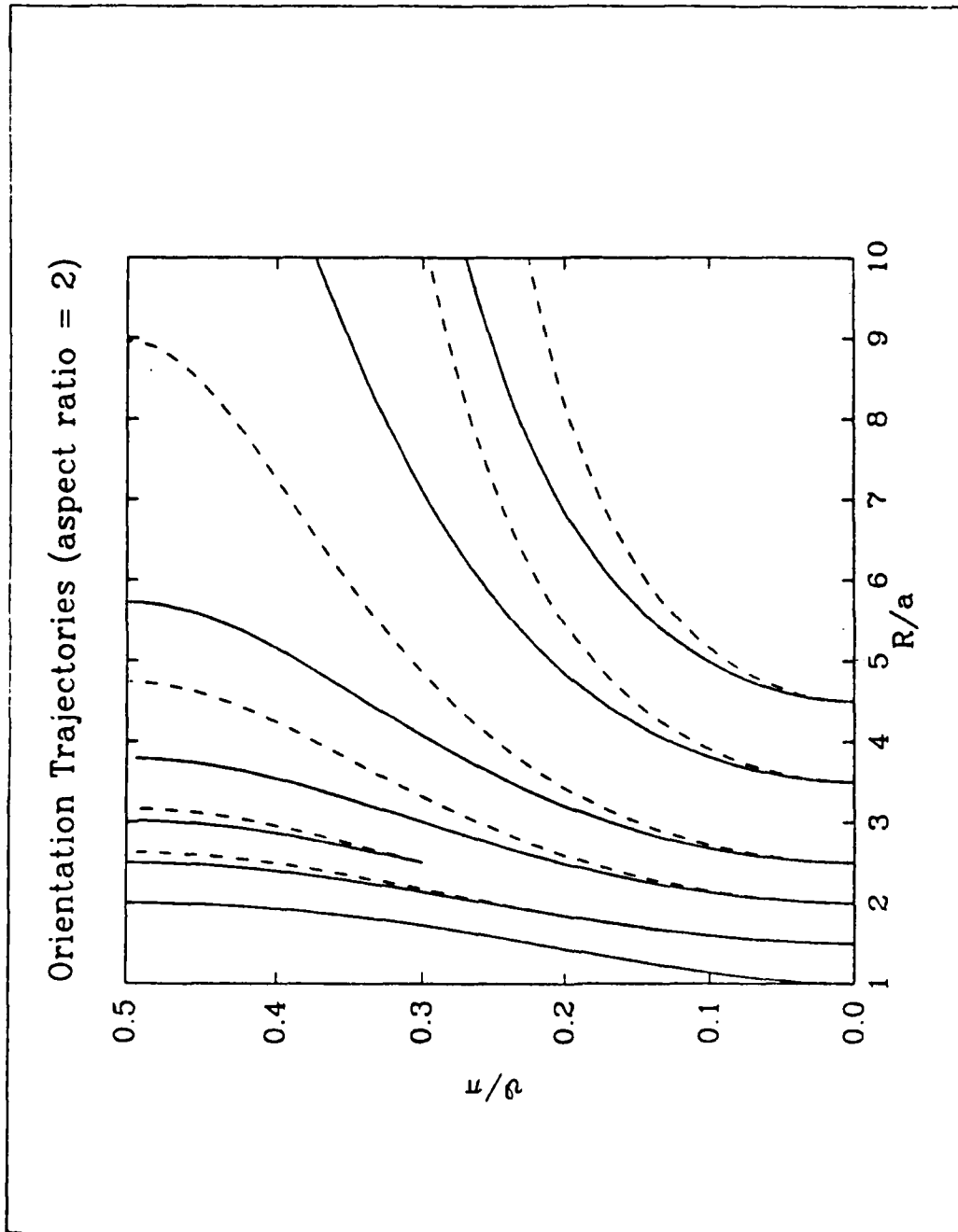


Figure 2. Evolution of orientation and separation between two spheroids, aspect ratio = 10, settling as in Figure 1. The solid and dashed trajectories are for oblate and prolate spheroids respectively. The separatrix goes through the x on the right border.

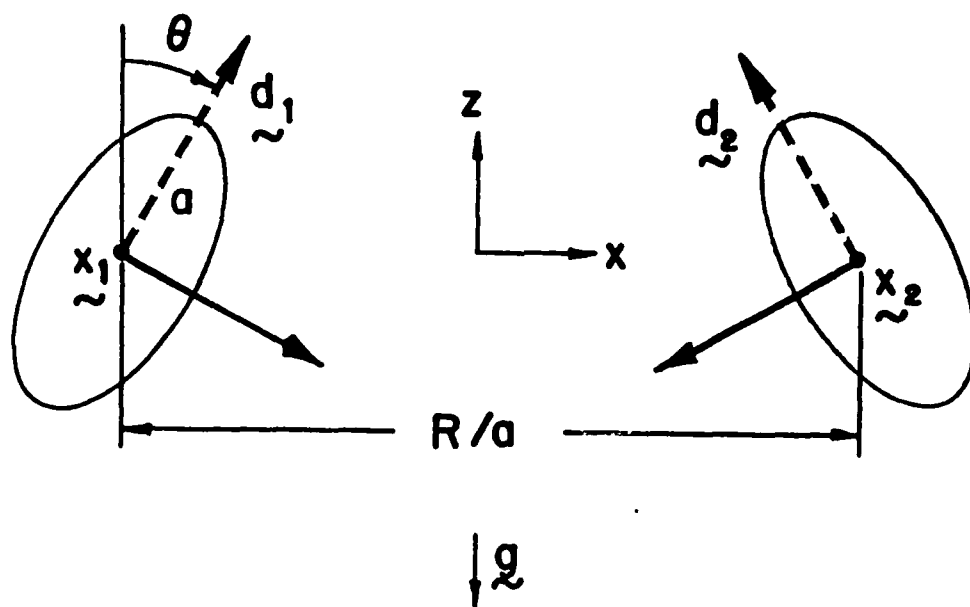


Figure 1. Mirror symmetry geometry of two inclined spheroids with their axes in a common plane. The solid and dashed axes are the symmetry axes for oblate and prolate spheroids, respectively

now consider two inclined oblate spheroids settling with their axes lying in a common vertical plane (Figure 1). At all times, the geometry is specified by the dimensionless center-to-center separation, R/a and θ , the polar angle⁴ between \underline{d}_1 and the x-axis. At all but small separations, the two-reflection solution provides accurate answers. The convergence behavior is similar to that reported in Kim (1985b) for prolate spheroids.

The evolution of the geometry is caused by the anisotropy in the mobility tensors and the rotation of the spheroids about the y-axis (which for oblate spheroid is co-incident with a major principal axis). Since the mobility is less in the axial than in the transverse direction, an inclined spheroid drifts horizontally as it settles. At the same time, the spheroid rotation changes the orientation of the axis. These two effects, under the quasi-steady assumption, are governed by the dimensionless equations (with R/a rewritten now as R)

$$\dot{\theta} = \omega_y(R, \theta) \quad (3.12)$$

$$\dot{R} = -2U_x(R, \theta) \quad (3.13)$$

Figures 2 and 3 show the evolution of R and θ as determined by integrating (3.12) and (3.13) with a fourth order Runge-Kutta routine. The solid lines are the new results for oblate spheroids and the dashed lines are the earlier results for prolate spheroids. The plots include the curve

$$R = 2(1 - e^2 \cos^2 \theta)^{1/2},$$

for contact between the two spheroids.

4. This θ differs from the one used in Kim (1985b) for prolate spheroids by $\pi/2$ in order that the same value of θ in the two problems yields identical cross-sections in the x-z plane.

The contributions to the sedimentation and angular velocities on ellipsoid 1 at the second reflection are obtained by using \underline{v}_{12} as the incident field in the Faxen laws. The method of reflections result for \underline{U}_1 is now accurate to $O(R^{-5})$. An error of $O(R^{-6})$ comes from the neglected quadrupole fields in \underline{v}_{12} (for which the Faxen laws are as yet unavailable). Thus the solution for ellipsoids has been developed to the same level as that presented for prolate spheroids in Kim (1985b).

It should be clear from the steps used at the first and second reflections that in general, at higher order reflections, the contribution to the sedimentation velocity of ellipsoid α from the n -th multipole from ellipsoid β is of the form:

$$\underline{L}_{\beta}^{(n)} \cdot \iiint_{E_{\alpha}} \iiint_{E_{\beta}} f_{(1)}(\underline{x}'_{\alpha}) f_{(n)}(\underline{x}'_{\beta}) \{1 + (\frac{1}{2}c_{\alpha}^2 q_{\alpha}^2 + c_{\beta}^2 q_{\beta}^2 / (4n-2)) \nabla^2\} \frac{\underline{I}(\underline{x}_{\alpha} - \underline{x}'_{\beta})}{(8\pi\mu)} dA_{\alpha} dA_{\beta},$$

where $\underline{L}_{\beta}^{(n)}$ is the appropriate multipole moment on ellipsoid β obtained at the previous reflection. An analogous procedure can be followed to determine the contribution to the angular velocity.

In actual computation, the integrals over the fundamental ellipses were parametrized with the elliptic coordinates:

$$x = a_E \rho \cos \phi, \quad y = b_E \rho \sin \phi.$$

Three-point Gaussian quadratures were adequate for the ρ -integration (the Gaussian quadratures were performed after the change of variable, $\tilde{\rho}^2 = 1 - \rho^2$). Simpson's rule was used for the ϕ -integration.

weighted by density functions which appear in the singularity solution of the conjugate boundary value problem.

3.1 Sedimentation of two ellipsoids

We proceed to solve the sedimentation problem for two ellipsoids by the method of reflections as an application of the general results of Section 2. The zero-th order solution at particle- α is simply the velocity field generated by an isolated ellipsoid subject to an external force \underline{F}_α . For example, at ellipsoid 2,

$$\underline{U}_2^{(0)} = (\mu \underline{A})^{-1} \cdot \underline{F}_2, \quad (3.10a)$$

$$\underline{v}_2 = \underline{F}_\alpha \cdot \iint_E f_{(1)}(x', y') \left\{ 1 + \frac{1}{2} c^2 q^2 \nabla^2 \right\} \underline{I}(\underline{x} - \underline{x}') / (8\pi\mu) dx' dy', \quad (3.10b)$$

(Each ellipsoidal particle in the suspension has its own fundamental ellipse and constants. This dependence is not expressed in order to simplify the notation). The contributions to the sedimentation and angular velocities on ellipsoid 1 from the first reflection, $\underline{U}_1^{(1)}$ and $\underline{\omega}_1^{(1)}$, are obtained by using $\underline{v}_2(\underline{x})$ as the incident field in the Faxen laws for the translational and rotational velocities on a force-free and torque-free ellipsoid. The leading term in the reflected field, \underline{v}_{21} , is a Stokes-dipole field,

$$\underline{v}_{21}(\underline{x}) = (\underline{S}_2^{(1)} \cdot \nabla) \cdot \iint_E f_{(2)}(x', y') \left\{ 1 + \frac{1}{6} c^2 q^2 \nabla^2 \right\} \underline{I}(\underline{x} - \underline{x}') / (8\pi\mu) dx' dy', \quad (3.11)$$

with the stresslet determined from the appropriate Faxen law, equation (3.9). The first reflection at ellipsoid 2 follows in a similar fashion, and the expression for the analogous dipole field, \underline{v}_{12} , is obtained by switching the particle labels.

$$\begin{aligned} \underline{T} = & \mu \underline{C} \cdot \iint_E f_{(2)}(x', y') \left[\frac{1}{2} \nabla \times \underline{v}^{\infty}(\underline{x}') - \underline{\omega} \right] dx' dy' \\ & + \mu \underline{H} : \iint_E f_{(2)}(x', y') \left\{ 1 + \frac{1}{6} c^2 q^2 \nabla^2 \right\} \underline{e}_{kl}^{\infty}(\underline{x}') dx' dy', \end{aligned} \quad (3.5)$$

$$\begin{aligned} S_{ij} = & \mu M_{ijkl} \iint_E f_{(2)}(x', y') \left\{ 1 + \frac{1}{6} c^2 q^2 \nabla^2 \right\} e_{kl}^{\infty}(\underline{x}') dx' dy' \\ & + \mu H_{k1j} \iint_E f_{(2)}(x', y') \left[\frac{1}{2} \nabla \times \underline{v}^{\infty}(\underline{x}') - \underline{\omega} \right]_k dx' dy'. \end{aligned} \quad (3.6)$$

For force-free and torque-free particles, these results can be rearranged into the following expressions for the translational velocity, rotational velocity and stresslet.

$$\underline{U} = \iint_E f_{(1)}(x', y') \left\{ 1 + \frac{1}{2} c^2 q^2 \nabla^2 \right\} \underline{v}^{\infty}(\underline{x}') dx' dy', \quad (3.7)$$

$$\omega_1 = \iint_E f_{(2)}(x', y') \left[\frac{1}{2} \nabla \times \underline{v}^{\infty}(\underline{x}') \right]_1 dx' dy' \quad (3.8)$$

$$\begin{aligned} & + (C^{-1})_{ij} H_{k1j} \iint_E f_{(2)}(x', y') \left\{ 1 + \frac{1}{6} c^2 q^2 \nabla^2 \right\} e_{kl}^{\infty}(\underline{x}') dx' dy' \\ S_{ij} = & \mu [M_{ijkl} - H_{mij} (C^{-1})_{mn} H_{nkl}] \end{aligned} \quad (3.9)$$

$$\times \iint_E f_{(2)}(x', y') \left\{ 1 + \frac{1}{6} c^2 q^2 \nabla^2 \right\} e_{kl}^{\infty}(\underline{x}') dx' dy'.$$

Equations (3.4) to (3.9) reduce to the appropriate Faxen laws for prolate spheroids derived by Kim (1985a) in the limit as $b \rightarrow c$.

Thus the force, torque and stresslet on an ellipsoidal particle in and ambient flow field \underline{v}^{∞} are obtained by integrating the ambient velocity, vorticity and rate-of-strain (respectively) over the fundamental ellipse,

3. FAXEN LAWS FOR ELLIPSOIDAL PARTICLES

A correspondence between singularity solutions and Faxen laws follows as a corollary of the Lorentz (1907) reciprocal theorem (Brenner 1964, Kim 1985a). The new forms of the Faxen laws obtained in this manner are more useful than earlier infinite series expansions derived by Brenner (1964) and Rallison (1978) when the higher order derivatives of the velocity field are not available.

The linear relations between the drag, torque and stresslet on the ellipsoid and the ambient field can be expressed as:

$$F_i = \mu A_{ij} (U^{\infty} - U)_j \quad (3.1)$$

$$T_i = \mu C_{ij} (\Omega^{\infty} - \omega)_j + \mu H_{ijk} E_{jk} \quad (3.2)$$

$$S_{ij} = \mu M_{ijkl} E_{kl} + \mu H_{kij} (\Omega^{\infty} - \omega)_k \quad (3.3)$$

where \underline{A} , \underline{B} , \underline{C} , \underline{H} and \underline{M} are material tensors whose components may be deduced from equations (2.9), (2.10) and (2.11). The Faxen relations are generalizations of (3.1), (3.2) and (3.3) since they give \underline{F} , \underline{T} and \underline{S} in any ambient velocity field that satisfies the Stokes equations over the unbounded domain. We apply the reciprocal theorem to the singularity solutions as shown in Kim (1985a) to obtain the following forms of the Faxen laws for the force, torque and stresslet:

$$\underline{F} = \mu \underline{A} \cdot \iint_E f_{(1)}(\underline{x}', y') \left\{ 1 + \frac{1}{2} c^2 q^2 \nabla^2 \right\} \underline{v}^{\infty}(\underline{x}') dx' dy' - \mu \underline{A} \cdot \underline{U}, \quad (3.4)$$

In summary, the basic results are:

- 1) The disturbance velocity field for a translating ellipsoid (or a fixed ellipsoid in a uniform stream) is generated by a distribution of stokeslets and potential doublets over the fundamental ellipse.
- 2) The disturbance fields for a rotating ellipsoid (or a fixed ellipsoid in a constant vorticity field) and for a stationary ellipsoid in a rate-of-strain field are generated by a distribution of rotlets, stresslets and Stokes-octupoles over the fundamental ellipse.
- 3) For prolate spheroids, the fundamental ellipse degenerates into a line segment from one focal point to the other and the singularity solutions of Chwang & Wu are recovered. For oblate spheroids, the fundamental ellipse degenerates into a circular disk with a diameter equal to the focal length of the ellipse of rotation.

In all cases, the density functions for the dominant singularities are similar to those which appear in analogous problems in potential theory.

obtained by evaluating the following harmonic functions at $\lambda=0$.³

$$\chi(\lambda) = abc \int_{\lambda}^{\infty} [P(\lambda)]^{-1} d\lambda, \quad (2.12)$$

$$\alpha(\lambda) = abc \int_{\lambda}^{\infty} [(a^2+\lambda)P(\lambda)]^{-1} d\lambda, \quad (2.13)$$

with $P(\lambda) = [(a^2+\lambda)(b^2+\lambda)(c^2+\lambda)]^{1/2}$

The lower limit of the definite integral, $\lambda(x,y,z)$, is the positive root of

$$\frac{x^2}{a^2+\lambda} + \frac{y^2}{b^2+\lambda} + \frac{z^2}{c^2+\lambda} = 1.$$

The functions $\beta(\lambda)$ and $\gamma(\lambda)$ are obtained by successive cycling of the dependence on a, b and c. The ' functions are defined by:

$$\alpha'(\lambda) = (\gamma - \beta)/(b^2 - c^2), \quad (2.14)$$

with $\beta'(\lambda)$ and $\gamma'(\lambda)$ defined by successive cycling of the dependence on a, b and c (and therefore also, α , β and γ). The " functions are defined by:

$$\alpha''(\lambda) = (b^2\beta - c^2\gamma)/(b^2 - c^2), \quad (2.15)$$

with $\beta''(\lambda)$ and $\gamma''(\lambda)$ defined by successive cycling of the dependence on a, b and c (and therefore also, α , β and γ). This completes the description of the singularity solution. For the special case of ellipsoids of revolution, these constants are given in the appendix along with a complete description of the resistance tensors. Asymptotic expressions for the spheroidal resistance functions are also provided for slender, flat and near-sphere limits.

3. α , β and γ are as defined in Happel & Brenner (1973) and differ from Jeffery's definition by a factor of (abc) . This also holds for the ' and " functions.

an elliptical disk, as can be seen by looking at the limit $c = 0$ in equation (2.7).

The function $q(x,y)$ which appears in $f_{(n)}$ plays a prominent role in the potential theory for ellipsoidal particles (see Miloh (1974)). In fact, in potential theory, q^{-1} is the requisite charge distribution over the fundamental ellipse which generates ellipsoidal equipotential surfaces. Chwang & Wu (1975) have noted that the distribution of Stokes multipoles in low-Reynolds-number problems is similar to the distribution of multipoles in analogous problems in potential theory, except for the presence of additional degenerate multipoles (the $\nabla^2 \underline{\underline{I}}$ term) in equation (2.7). The presence of such quadrupoles (or potential doublet) when $n=1$ and octupoles when $n=2$ in (2.7) are consistent with (and in fact extend) the rules stated by Chwang & Wu (1975) for prolate spheroids.

To complete the solution, we must relate $\underline{\underline{F}}$, $\underline{\underline{T}}$ and $\underline{\underline{S}}$ in terms of the knowns, $\underline{\underline{U}} - \underline{\underline{U}}$, $\underline{\underline{\Omega}} - \underline{\underline{\omega}}$ and $\underline{\underline{E}}$. These relations are found in Oberbeck (1876) and Jeffery (1922), some of which are shown below. Expressions for other components can be obtained by the well known mnemonic of cycling the subscripts x , y and z , and the dependence on a , b and c .

$$F_x = 16\pi\mu abc(\chi_0 + \alpha_0 a^2)^{-1}(U_x^\infty - U_x) \quad (2.9)$$

$$T_x = \frac{16}{3}\pi\mu abc(b^2\beta_0 + c^2\gamma_0)^{-1}[(b^2+c^2)(\Omega_x^\infty - \omega_x) + (b^2-c^2)\frac{1}{2}(E_{yz} + E_{zy})] \quad (2.10)$$

$$S_{xx} = \frac{16}{9}\pi\mu abc(2\alpha_0''E_{xx} - \beta_0''E_{yy} - \gamma_0''E_{zz})(\beta_0''\gamma_0'' + \gamma_0''\alpha_0'' + \alpha_0''\beta_0'')^{-1} \quad (2.11a)$$

$$S_{xy} = S_{yx} = \frac{8}{3}\pi\mu abc(a^2\alpha_0 + b^2\beta_0)^{-1} \quad (2.11b)$$

$$\times [(a^2-b^2)(\Omega_z^\infty - \omega_z) + (\alpha_0 + \beta_0)[\gamma_0']^{-1}\frac{1}{2}(E_{xy} + E_{yx})].$$

Here, χ_0 , α_0 , β_0 , γ_0 , α_0' , β_0' , γ_0' , α_0'' , β_0'' and γ_0'' are constants which are

first consider $\underline{L}^{(n)}$, the vector operator. For $n=1$, $\underline{L}^{(1)} \cdot \underline{I} = -\underline{F} \cdot \underline{I}$, the Stokes monopole field, where \underline{F} is the force exerted on the ellipsoid by the fluid, i.e.

$$\oint \underline{q} \cdot \underline{n} \, dA$$

For $n=2$, $\underline{L}^{(2)} \cdot \underline{I} = [(\underline{S} + \underline{T}) \cdot \underline{V}] \cdot \underline{I}$ is the Stokes dipole field, where \underline{S} and \underline{T} are the symmetric and anti-symmetric parts of the stress-dipole on the ellipsoid,

$$\oint (\underline{q} \cdot \underline{n}) \underline{x} \, dA$$

\underline{S} is called the stresslet in Batchelor & Green (1972)¹. \underline{T} is related to the torque exerted on the ellipsoid by the fluid, by the usual relation between anti-symmetric dyadics and pseudo-vectors,

$$T_{ij} = -\frac{1}{2} \epsilon_{ijk} T_k.$$

$E(x', y')$, the integration domain, is the interior of the fundamental ellipse,

$$\frac{x^2}{a_E^2} + \frac{y^2}{b_E^2} = 1, \quad z = 0.$$

The fundamental ellipse is the degenerate elliptical disk in a family of confocal ellipsoids. The major and minor semi-axes of the fundamental ellipse, a_E and b_E , are given in equation (2.8c)². The density function $f_{(n)}(x', y')$ in $E(x', y')$ is physically the surface singularity distribution for

-
1. The isotropic part of the symmetric stress-dipole usually has no physical significance. Batchelor and Green (1972) remove this degree of freedom by setting the trace of the stresslet to zero.
 2. Hobson (1955) and Miloh (1974) use k and $(k^2 - h^2)^{1/2}$ in place of our a_E and b_E .

- Hinch, E.J. & Leal, L.G. 1972 The effect of Brownian motion on the rheological properties of a suspension of non-spherical particles. J. Fluid Mech. 52, 683-712.
- Hinch, E.J. 1977 An averaged-equation approach to particle interactions in a fluid suspension. J. Fluid Mech. 83, 695-720.
- Hobson, E.W. 1955 The theory of spherical and ellipsoidal harmonics. Chelsea.
- Jeffery, G.B. 1922 The motion of ellipsoidal particles immersed in a viscous fluid. Proc. Roy. Soc. A102, 161-179.
- Jeffrey, D.J. & Onishi, Y. 1984 Calculation of the resistance and mobility functions for two unequal rigid spheres in low-Reynolds-number flow. J. Fluid Mech. 139, 261-290.
- Kellogg, O.D. 1953 Foundations of potential theory. Dover, New York.
- Kim, S. 1985 A note on Faxen laws for nonspherical particles. Int. J. Multiphase Flow (in press).
- Kim, S. 1985 Sedimentation of two arbitrarily oriented spheroids in a viscous fluid. Int. J. Multiphase Flow (in press).
- Liao, W. & Krueger, D.A. 1980 Multipole expansion calculation of slow viscous flow about spheroids of different sizes. J. Fluid Mech. 96, 223-241.
- Lorentz, H.A. 1897 A general theorem concerning the motion of a viscous fluid and a few consequences derived from it. Versl. Kon. Akad. Wet. Amst. 5, 168-175.
- Lorentz, H.A. 1907 A general theorem concerning the motion of a viscous fluid. Abandl. Theoret. Phys. 1, 23-31.
- Miloh, T. 1974 The ultimate image singularities for external ellipsoidal harmonics. SIAM J. Appl. Math. 26, 334-344.
- Oberbeck, A. 1876 Ueber stationären Flüssigkeitsbewegungen mit Berücksichtigung der inneren Reibung. J. reine. angew. Math. 81, 62-80.
- Oseen, C.W. 1927 Hydrodynamik. Leipzig: Akad. Verlagsgesellschaft.
- Rallison, J.M. 1978 Note on the Faxen relations for a particle in Stokes flow. J. Fluid Mech. 88, 529-533.
- Smoluchowski, M. 1911 On the mutual action of spheres which move in a viscous liquid. Bull. Acad. Sci. Cracovie 1A, 28-39.
- Tuck, E.O. 1964 Some methods for flow past blunt slender bodies. J. Fluid Mech. 18, 619-635.
- Wakiya, S. 1965 Mutual interaction of two spheroids sedimenting in a viscous fluid. J. Phys. Soc. Jap. 20, 1502-1514.

Appendix 1. DERIVATION OF THE SINGULARITY SOLUTION

We show here that the singularity solution, equation (2.7), is equivalent to the solutions obtained by Oberbeck (1876) and Jeffery (1922), i.e., the solutions obtained by separation of variables in ellipsoidal coordinates.

The proof is simple once certain integral representations for $\chi(\lambda)$ and $\Omega(\lambda)$, the Dirchlet gravitational potential for a solid ellipsoid, are established. The Dirchlet potential is defined by^a:

$$\Omega(\lambda) = \pi abc \int_{\lambda}^{\infty} \left(\frac{x^2}{a^2+\lambda} + \frac{y^2}{b^2+\lambda} + \frac{z^2}{c^2+\lambda} - 1 \right) \frac{d\lambda}{P}, \quad (\text{A.1})$$

The lower limit of the definite integral, $\lambda(x,y,z)$, is as defined earlier.

The required integral representations are:

$$\chi = 2abc \iint_E f_{(1)}(x',y') \frac{1}{|\underline{x}-\underline{x}'|} dx'dy', \quad (\text{A.2})$$

$$\Omega = -4\pi abc \iint_E f_{(1)}(x',y') q^2(x'y') \frac{1}{|\underline{x}-\underline{x}'|} dx'dy', \quad (\text{A.3})$$

with $f_{(1)}$ given by equation (2.8a).

The integral representation for χ is derived in Miloh (1974) in the more general setting of representation theorems for external Lamé functions^b, F_n^m . The harmonic χ is related to the Lamé functions by $\chi(\lambda) = 2abcF_0^0(\rho)$ with $\rho^2 = a^2 + \lambda$. The integral representation for Ω follows from the representation for χ . From Kellogg (1953),

$$\Omega = -2\pi \int_0^1 \chi(\lambda;u)/u du. \quad (\text{A.4})$$

The parameter u is introduced by replacing a , b and c in the expression for χ

a. This definition is the same as in Happel & Brenner (1973) but differs from Jeffery's by a factor of πabc .

b. These functions are defined in the extensive treatise by Hobson (1955).

with u_a , u_b and u_c . According to (A.4), Ω is a superposition of χ functions for a family of ellipsoids imbedded inside the original ellipsoid. This representation is one way of demonstrating that Ω is a harmonic. The desired result, (A.3), can be obtained by inserting (A.2) into (A.4) and performing the u -integration first.

We are now in a position to recover Oberbeck's solution as given by equation (5-11.8) in Happel and Brenner (1973) for an ellipsoid in a uniform stream (streaming in the x -direction with velocity U^∞):

$$\begin{aligned} v_x &= -\frac{a^2}{2\pi} U^\infty (\chi_0 + \alpha_0 a^2)^{-1} \frac{\partial^2 \Omega}{\partial x^2} + U^\infty (\chi_0 + \alpha_0 a^2)^{-1} \left(x \frac{\partial \chi}{\partial x} - \chi \right) + U^\infty \\ v_y &= -\frac{a^2}{2\pi} U^\infty (\chi_0 + \alpha_0 a^2)^{-1} \frac{\partial^2 \Omega}{\partial x \partial y} + U^\infty (\chi_0 + \alpha_0 a^2)^{-1} x \frac{\partial \chi}{\partial y} \\ v_z &= -\frac{a^2}{2\pi} U^\infty (\chi_0 + \alpha_0 a^2)^{-1} \frac{\partial^2 \Omega}{\partial x \partial z} + U^\infty (\chi_0 + \alpha_0 a^2)^{-1} x \frac{\partial \chi}{\partial z} \end{aligned} \quad (A.5)$$

The distribution of Stokeslets, $I_{ij}(\underline{x}-\underline{x}')$, in the singularity solution can be decomposed as

$$I_{ij}(\underline{x}-\underline{x}') = -\left(x_j \frac{\partial r^{-1}}{\partial x_1} - \frac{1}{r} \delta_{ij} \right) + x'_j \frac{\partial r^{-1}}{\partial x_1}, \quad \text{with } r = |\underline{x}-\underline{x}'|. \quad (A.6)$$

The χ -term in Oberbeck's solution is obtained by taking the first term on the right-hand-side of (A.6) and recognizing that the integral over the fundamental ellipse in (2.7) is precisely the integral representation for χ , equation (A.2). It is not difficult to show that the integral of the remaining term on the right-hand-side of (A.6) over the fundamental ellipse is related to the second derivatives of Ω , i.e.,

$$4\pi abc \iint_E f_{(1)}(x', y') x'_j \frac{\partial}{\partial x_1} \frac{1}{|\underline{x}-\underline{x}'|} dx' dy' = (a_j^2 - c^2) \frac{\partial^2 \Omega}{\partial x_1 \partial x_j}. \quad (A.7)$$

with the temporary notation, $a_1=a$, $a_2=b$ and $a_3=c$. This completes the transformation of the Stokeslet distribution.

The potential doublet satisfies

$$\nabla^2 \underline{I} = -2\nabla\nabla(r^{-1})$$

for $r \neq 0$. Therefore, the integral of the potential doublet over the fundamental ellipse in (2.7) is just the second derivative of the integral representation for Ω . Thus the Ω -terms in Oberbeck's solution are obtained by combining (A.7) and the distribution of potential doublets in (2.7).

By a similar albeit more tedious procedure, one can relate the $n=2$ case in the singularity solution to Jeffery's (1922) solution for rotation and rate-of-strain. Readers are referred to the (1922) paper for the details of the ellipsoidal-coordinate solution. In his equations (18), (19) and (20) for the velocity components, the terms containing the constants A, B, C, F, F', G, G', H and H' may be rearranged into the stresslet and rotlet distributions of equation (2.7) plus octupoles of strength $(a_j^2 - c^2)$. After some lengthy algebraic rearrangement^c, these octupoles and the terms containing the constants R, S, T, U, V and W in the (1922) paper (these terms satisfy $\nabla^2 \underline{y} = 0$) reduce to the octupoles in equation (2.7).

c. These steps are omitted here but are available from the author.

Appendix 2. COLLECTION OF RESULTS FOR ELLIPSOIDS OF REVOLUTION

The scalar coefficients which arise in the solution of the resistance problems for ellipsoids of revolution are scattered throughout the literature. Here, the complete set of resistance coefficients for both prolate and oblate spheroids are furnished for the convenience of the reader in Tables 1-3. The information is grouped as follows:

- 1) The expressions for the ellipsoidal constants, $\alpha_0, \beta_0, \dots, \gamma_0^n$ in the limit of oblate and prolate spheroids, are given in Table 1.
- 2) The definitions of and expressions for the eight resistance functions which relate the force, torque and stresslet on oblate and prolate spheroids to the net translation, net rotation and ambient rate-of-strain are given in Table 2. Following Chwang & Wu (1975), the shape-dependence is expressed in terms of the eccentricity, e , of the generating ellipse.
- 3) In Table 3, asymptotic formulae are given for all eight functions in the limit as $e \rightarrow 0$ (near-spheres) and $e \rightarrow 1$ (flat disks and thin needles).

The notation for the resistance functions follows that used by Jeffrey & Onishi (1984). The letters X, Y and Z are assigned according to $m = 0, 1$ and 2 respectively, where m is the azimuthal constant which appears in boundary condition. Superscripts A, C, H and M indicate the relation with the appropriate resistance tensor. The form taken by tensors A and C in Table 2 is simply the decomposition of the translation and rotation problems into motions parallel and perpendicular to the axis of symmetry. The form taken by M is also a consequence of the particle symmetry. Finally, as a consequence of the Lorentz reciprocal theorem, γ^H appears both as the torque on a spheroid in a rate-of-strain field and also as the stresslet on a rotating spheroid as shown by Hinch (1972).

The exact and asymptotic formulae for the resistance functions are plotted in Figures (4a) to (5h), from which it is apparent that the asymptotic forms are accurate over a wide range of aspect ratios. Rather curiously, for a flat disk, all three torque functions, X^Z, Y^C and γ^H are equal (and nonzero)

Prolate Spheroids (a > b = c)

$$\chi_0 = \frac{a^2(1-e^2)}{e} \log\left(\frac{1+e}{1-e}\right)$$

$$\alpha_0 = \frac{(1-e^2)}{e^3} \log\left(\frac{1+e}{1-e}\right) - \frac{2(1-e^2)}{e^2}$$

$$\gamma_0 = \frac{1}{c^2} - \frac{(1-e^2)}{2e^3} \log\left(\frac{1+e}{1-e}\right)$$

$$\alpha_0' = \frac{1}{a^2} \left\{ \frac{5e^2-3}{4e^4(1-e^2)} + \frac{3(1-e^2)}{8e^5} \log\left(\frac{1+e}{1-e}\right) \right\}$$

$$\gamma_0' = \frac{1}{ae^2} \left\{ 3e-2e^3 - \frac{3}{2}(1-e^2) \log\left(\frac{1+e}{1-e}\right) \right\}$$

$$\alpha_0'' = \frac{3-e^2}{4e^4} - \frac{(1-e^2)(e^2+3)}{8e^5} \log\left(\frac{1+e}{1-e}\right)$$

$$\gamma_0'' = \frac{(1-e^2)}{e^5} \left\{ -3e + \frac{1}{2}(3-e^2) \log\left(\frac{1+e}{1-e}\right) \right\}$$

Oblate Spheroids (a = b > c)

$$\chi_0 = 2a^2 \frac{\sqrt{1-e^2}}{e} \cot^{-1}\left(\frac{\sqrt{1-e^2}}{e}\right)$$

$$\alpha_0 = \frac{\sqrt{1-e^2}}{e^3} \cot^{-1}\left(\frac{\sqrt{1-e^2}}{e}\right) - \frac{(1-e^2)}{e^2}$$

$$\gamma_0 = \frac{2}{e^2} - \frac{2\sqrt{1-e^2}}{e^3} \cot^{-1}\left(\frac{\sqrt{1-e^2}}{e}\right)$$

$$\alpha_0' = \frac{1}{a^2} \left\{ \frac{3-e^2}{e^4} - \frac{3\sqrt{1-e^2}}{e^5} \cot^{-1}\left(\frac{\sqrt{1-e^2}}{e}\right) \right\}$$

$$\gamma_0' = \frac{1}{a^2} \left\{ \frac{(1-e^2)(e^2-3)}{4e^4} + \frac{3\sqrt{1-e^2}}{4e^5} \cot^{-1}\left(\frac{\sqrt{1-e^2}}{e}\right) \right\}$$

$$\alpha_0'' = -\frac{3(1-e^2)}{e^4} + \frac{(3-2e^2)\sqrt{1-e^2}}{e^5} \cot^{-1}\left(\frac{\sqrt{1-e^2}}{e}\right)$$

$$\gamma_0'' = \frac{(1-e^2)(3-2e^2)}{4e^4} - \frac{(3-4e^2)\sqrt{1-e^2}}{4e^5} \cot^{-1}\left(\frac{\sqrt{1-e^2}}{e}\right)$$

Table 1. Ellipsoidal constants in the limit of prolate and oblate spheroidal cases
($\beta = \gamma$ for prolate spheroids and $\beta = \alpha$ for oblate spheroids).

Table 2

$$F_i = 6\pi\mu a \{X^A d_i d_j + Y^A (\delta_{ij} - d_i d_j)\} (U^\infty - U)_j$$

$$T_i = 8\pi\mu a^3 \{X^C d_i d_j + Y^C (\delta_{ij} - d_i d_j)\} (\Omega^\infty - \omega)_j$$

$$+ 8\pi\mu a^3 Y^H \frac{1}{2} (\epsilon_{ijl} d_k + \epsilon_{ikl} d_j) d_l E_{jk}$$

$$S_{ij} = \frac{20}{3} \pi\mu a^3 \{X^M d_{ijkl}^{(1)} + Y^M d_{ijkl}^{(2)} + Z^M d_{ijkl}^{(3)}\} E_{kl}$$

$$+ \frac{20}{3} \pi\mu a^3 \left(\frac{6}{5} Y^H\right) \frac{1}{2} (d_i \epsilon_{jkl} + d_j \epsilon_{ikl}) d_k (\Omega^\infty - \omega)_l$$

$$d_{ijkl}^{(1)} = \frac{3}{2} (d_i d_j - \frac{1}{3} \delta_{ij}) (d_k d_l - \frac{1}{3} \delta_{kl})$$

$$d_{ijkl}^{(2)} = \frac{1}{2} (d_i \delta_{jl} d_k + d_j \delta_{il} d_k + d_i \delta_{jk} d_l + d_j \delta_{ik} d_l - 4d_i d_j d_k d_l)$$

$$d_{ijkl}^{(3)} = \frac{1}{2} (\delta_{ik} \delta_{jl} + \delta_{jk} \delta_{il} - \delta_{ij} \delta_{kl} + d_i d_j \delta_{kl} + \delta_{ij} d_k d_l$$

$$- d_i \delta_{jl} d_k - d_j \delta_{il} d_k - d_i \delta_{jk} d_l - d_j \delta_{ik} d_l + d_i d_j d_k d_l)$$

Table 2 (continued)

Resistance Functions for Oblate Spheroids

$$X^A = \frac{8}{3} e^3 \left[2(2e^2-1) \cot^{-1} \left(\frac{\sqrt{1-e^2}}{e} \right) + 2e\sqrt{1-e^2} \right]^{-1}$$

$$Y^A = \frac{8}{3} e^3 \left[(2e^2+1) \cot^{-1} \left(\frac{\sqrt{1-e^2}}{e} \right) - e\sqrt{1-e^2} \right]^{-1}$$

$$X^C = \frac{2}{3} e^3 \left[\cot^{-1} \left(\frac{\sqrt{1-e^2}}{e} \right) - e\sqrt{1-e^2} \right]^{-1}$$

$$Y^C = \frac{2}{3} e^3 (2-e^2) \left[e\sqrt{1-e^2} - (1-2e^2) \cot^{-1} \left(\frac{\sqrt{1-e^2}}{e} \right) \right]^{-1}$$

$$Y^H = \frac{2}{3} e^5 \left[e\sqrt{1-e^2} - (1-2e^2) \cot^{-1} \left(\frac{\sqrt{1-e^2}}{e} \right) \right]^{-1}$$

$$X^M = \frac{4}{15} e^5 \left[(3-2e^2) \cot^{-1} \left(\frac{\sqrt{1-e^2}}{e} \right) - 3e\sqrt{1-e^2} \right]^{-1}$$

$$Y^M = \frac{2}{5} e^5 \left[e(1+e^2) - \sqrt{1-e^2} \cot^{-1} \left(\frac{\sqrt{1-e^2}}{e} \right) \right]$$

$$x \left\{ \left[3e-e^3 - 3\sqrt{1-e^2} \cot^{-1} \left(\frac{\sqrt{1-e^2}}{e} \right) \right] \left[e\sqrt{1-e^2} - (1-2e^2) \cot^{-1} \left(\frac{\sqrt{1-e^2}}{e} \right) \right] \right\}^{-1}$$

$$Z^M = \frac{8}{5} e^5 \left[3 \cot^{-1} \left(\frac{\sqrt{1-e^2}}{e} \right) - (2e^3+3e) \sqrt{1-e^2} \right]^{-1}$$

Table 2 (continued)

Resistance Functions for Prolate Spheroids

$$X^A = \frac{8}{3} e \alpha_1(e) = \frac{8}{3} e^3 \left[-2e + (1+e^2) \log\left(\frac{1+e}{1-e}\right) \right]^{-1}$$

$$Y^A = \frac{8}{3} e \alpha_2(e) = \frac{16}{3} e^3 \left[2e + (3e^2-1) \log\left(\frac{1+e}{1-e}\right) \right]^{-1}$$

$$X^C = \frac{4}{3} e^3 \gamma(e) = \frac{4}{3} e^3 (1-e^2) \left[2e - (1-e^2) \log\left(\frac{1+e}{1-e}\right) \right]^{-1}$$

$$Y^C = \frac{4}{3} e^3 \gamma'(e) = \frac{4}{3} e^3 (2-e^2) \left[-2e + (1+e^2) \log\left(\frac{1+e}{1-e}\right) \right]^{-1}$$

$$Y^H = -\frac{4}{3} e^5 \left[-2e + (1+e^2) \log\left(\frac{1+e}{1-e}\right) \right]^{-1}$$

$$X^M = \frac{8}{15} e^5 \left[(3-e^2) \log\left(\frac{1+e}{1-e}\right) - 6e \right]^{-1}$$

$$Y^M = \frac{4}{5} e^5 \left[2e(1-2e^2) - (1-e^2) \log\left(\frac{1+e}{1-e}\right) \right]$$

$$\times \left\{ \left[2e(2e^2-3) + 3(1-e^2) \log\left(\frac{1+e}{1-e}\right) \right] \left[-2e + (1+e^2) \log\left(\frac{1+e}{1-e}\right) \right] \right\}^{-1}$$

$$Z^M = \frac{16}{5} e^5 (1-e^2) \left[3(1-e^2)^2 \log\left(\frac{1+e}{1-e}\right) - 2e(3-5e^2) \right]^{-1}$$

Table 2. The resistance functions for oblate and prolate spheroids (scaled to the spherical result), as a function of e , the eccentricity of the generating ellipse. The constants $\alpha_1(e)$, $\alpha_2(e)$, $\gamma(e)$ and $\gamma'(e)$ are as in Chwang & Wu (1975).

Table 3

Asymptotic Behavior of Oblate Functions

<u>As $e \rightarrow 0$</u>	<u>As $e \rightarrow 1$ $\epsilon = \sqrt{1-e^2}$</u>
$X^A = (1 - \frac{1}{10} e^2 - \frac{31}{1400} e^4)$	$\frac{8}{3\pi} (1 + \frac{1}{2} \epsilon^2)$
$Y^A = (1 - \frac{1}{5} e^2 - \frac{79}{1400} e^4)$	$\frac{16}{9\pi} (1 + \frac{8}{3\pi} \epsilon - \frac{(15\pi^2-128)}{18\pi^2} \epsilon^2)$
$X^C = (1 - \frac{3}{10} e^2 - \frac{99}{1400} e^4)$	$\frac{4}{3\pi} (1 + \frac{4}{\pi} \epsilon + \frac{(32-3\pi^2)}{2\pi^2} \epsilon^2)$
$Y^C = (1 - \frac{3}{5} e^2 + \frac{39}{1400} e^4)$	$\frac{4}{3\pi} (1 + \frac{3}{2} \epsilon^2)$
$Y^H = 0 + \frac{1}{2} e^2 (1 - \frac{1}{10} e^2 - \frac{31}{1400} e^4)$	$\frac{4}{3\pi} (1 - \frac{1}{2} \epsilon^2)$
$X^M = (1 - \frac{9}{14} e^2 - \frac{13}{392} e^4)$	$\frac{8}{15\pi} (1 + \frac{8}{\pi} \epsilon + \frac{(128-9\pi^2)}{2\pi^2} \epsilon^2)$
$Y^M = (1 - \frac{4}{7} e^2 - \frac{173}{5880} e^4)$	$\frac{4}{5\pi} (1 + \frac{\pi}{2} \epsilon + \frac{(3\pi^2-20)}{8} \epsilon^2)$
$Z^M = (1 - \frac{5}{14} e^2 - \frac{95}{1176} e^4)$	$\frac{16}{15\pi} (1 + \frac{16}{3\pi} \epsilon + \frac{(512-45\pi^2)}{18\pi^2} \epsilon^2)$

Table 3 (continued)

Asymptotic Behavior of Prolate Functions

<u>As $e \rightarrow 0$</u>	<u>As $e \rightarrow 1$ $\epsilon = \sqrt{1-e^2}$ $L_\epsilon = \log\left(\frac{2}{\epsilon}\right)$</u>
$X^A = 1 - \frac{2}{5} e^2 - \frac{17}{175} e^4$	$X^A = \frac{4}{6L_\epsilon - 3} - \frac{(8L_\epsilon - 6)\epsilon^2}{12L_\epsilon^2 - 12L_\epsilon + 3}$
$Y^A = 1 - \frac{3}{10} e^2 - \frac{57}{700} e^4$	$Y^A = \frac{8}{6L_\epsilon + 3} - \frac{4\epsilon^2}{12L_\epsilon^2 + 12L_\epsilon + 3}$
$X^C = 1 - \frac{6e^2}{5} + \frac{27}{175} e^4$	$X^C = 0 + \frac{2}{3} \epsilon^2 + \frac{(2L_\epsilon - 2)\epsilon^4}{3}$
$Y^C = 1 - \frac{9}{10} e^2 + \frac{18}{175} e^4$	$Y^C = \frac{2}{6L_\epsilon - 3} + \frac{\epsilon^2}{12L_\epsilon^2 - 12L_\epsilon + 3}$
$Y^H = -\frac{1}{2} e^2 + \frac{1}{5} e^4$	$Y^H = -\frac{2}{6L_\epsilon - 3} + \frac{(8L_\epsilon - 5)\epsilon^2}{12L_\epsilon^2 - 12L_\epsilon + 3}$
$X^M = 1 - \frac{6}{7} e^2 + \frac{1}{49} e^4$	$X^M = \frac{4}{30L_\epsilon - 45} - \frac{(24L_\epsilon - 26)\epsilon^2}{60L_\epsilon^2 - 180L_\epsilon + 135}$
$Y^M = 1 - \frac{13}{14} e^2 + \frac{44}{735} e^4$	$Y^M = \frac{2}{10L_\epsilon - 5} + \frac{(16L_\epsilon^2 - 32L_\epsilon + 13)\epsilon^2}{20L_\epsilon^2 - 20L_\epsilon + 5}$
$Z^M = 1 - \frac{8}{7} e^2 + \frac{17}{147} e^4$	$Z^M = 0 + \frac{4}{5} \epsilon^2 + \frac{2}{5} \epsilon^4$

Table 3. Asymptotic behavior of the spheroidal resistance functions in the limit of spheres, needles and disks.

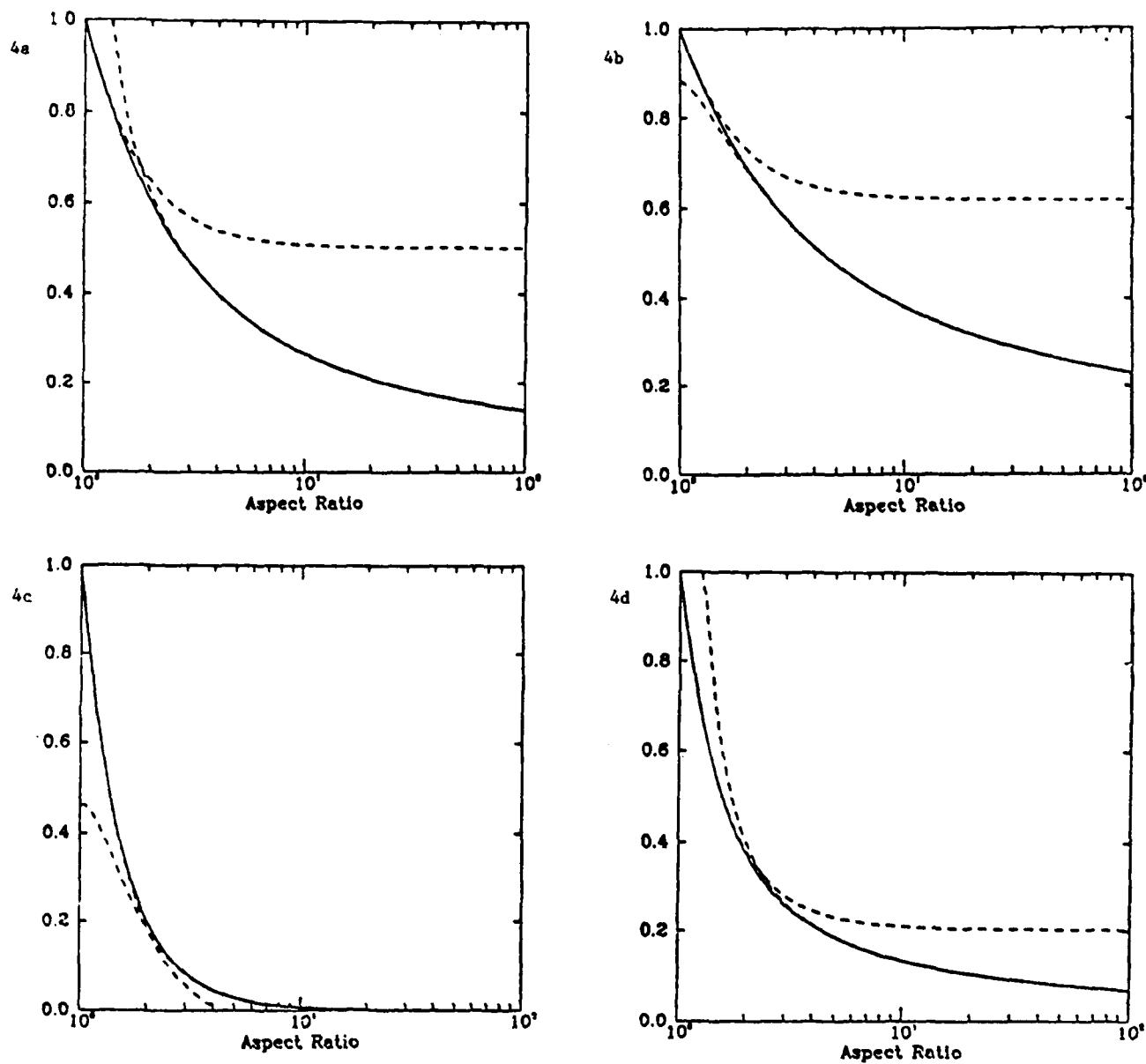


Figure 4. The resistance functions for oblate spheroids, scaled by the results for spheres. The dashed curves are the asymptotic forms of Table 3.

- Force/translation (parallel to axis) function X^A .
- Force/translation (perpendicular to axis) function Y^A .
- Torque/rotation (parallel to axis) function X^C .
- Torque/rotation (perpendicular to axis) function Y^C .

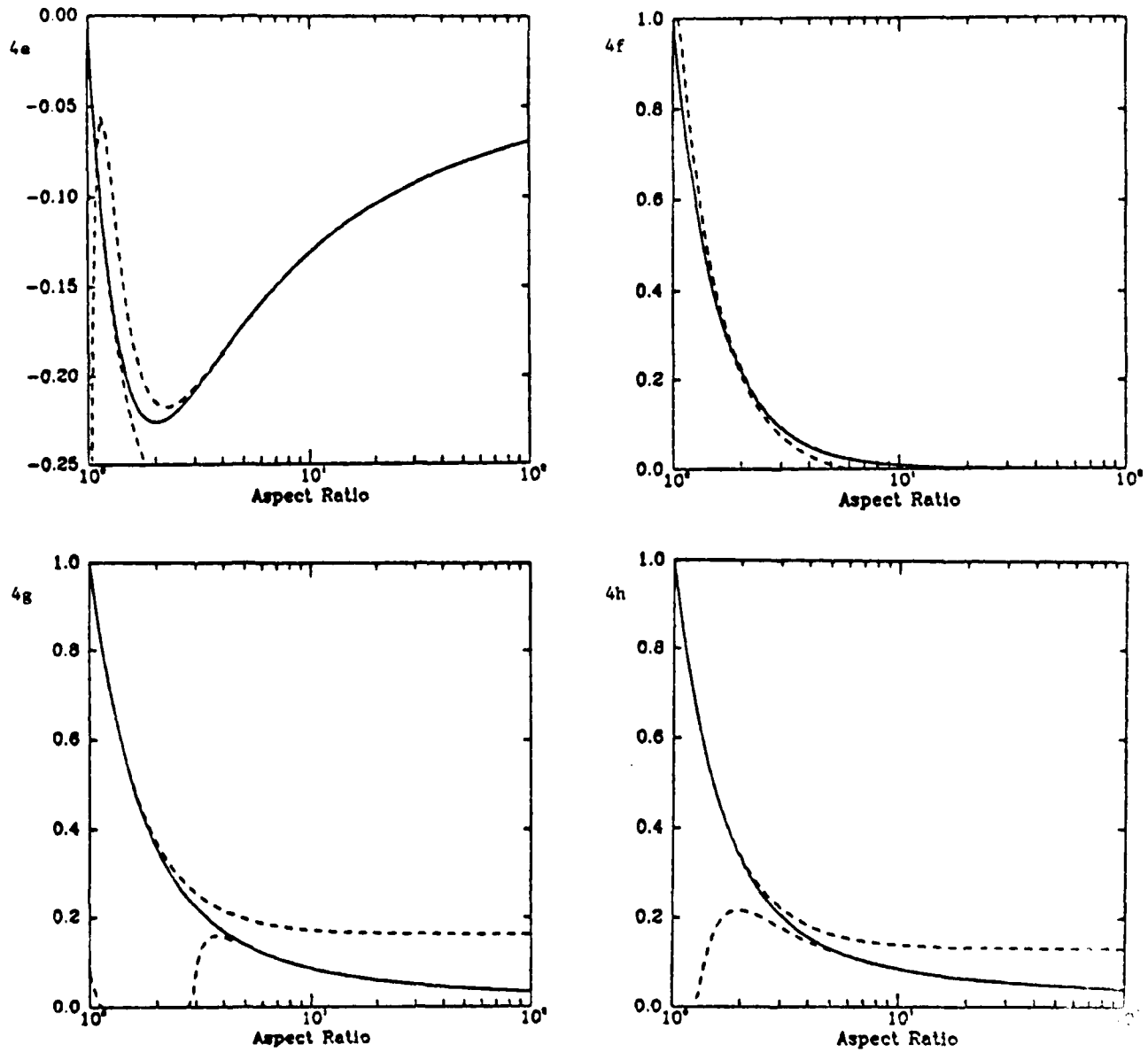


Figure 4. (Continued)

- e. Torque/rate-of-strain function Y^H .
- f. Stresslet/rate-of-strain (axisymmetric straining) function X^M .
- g. Stresslet/rate-of-strain (hyperbolic straining) function Y^M .
- h. Stresslet/rate-of-strain (hyperbolic straining) function Z^M .

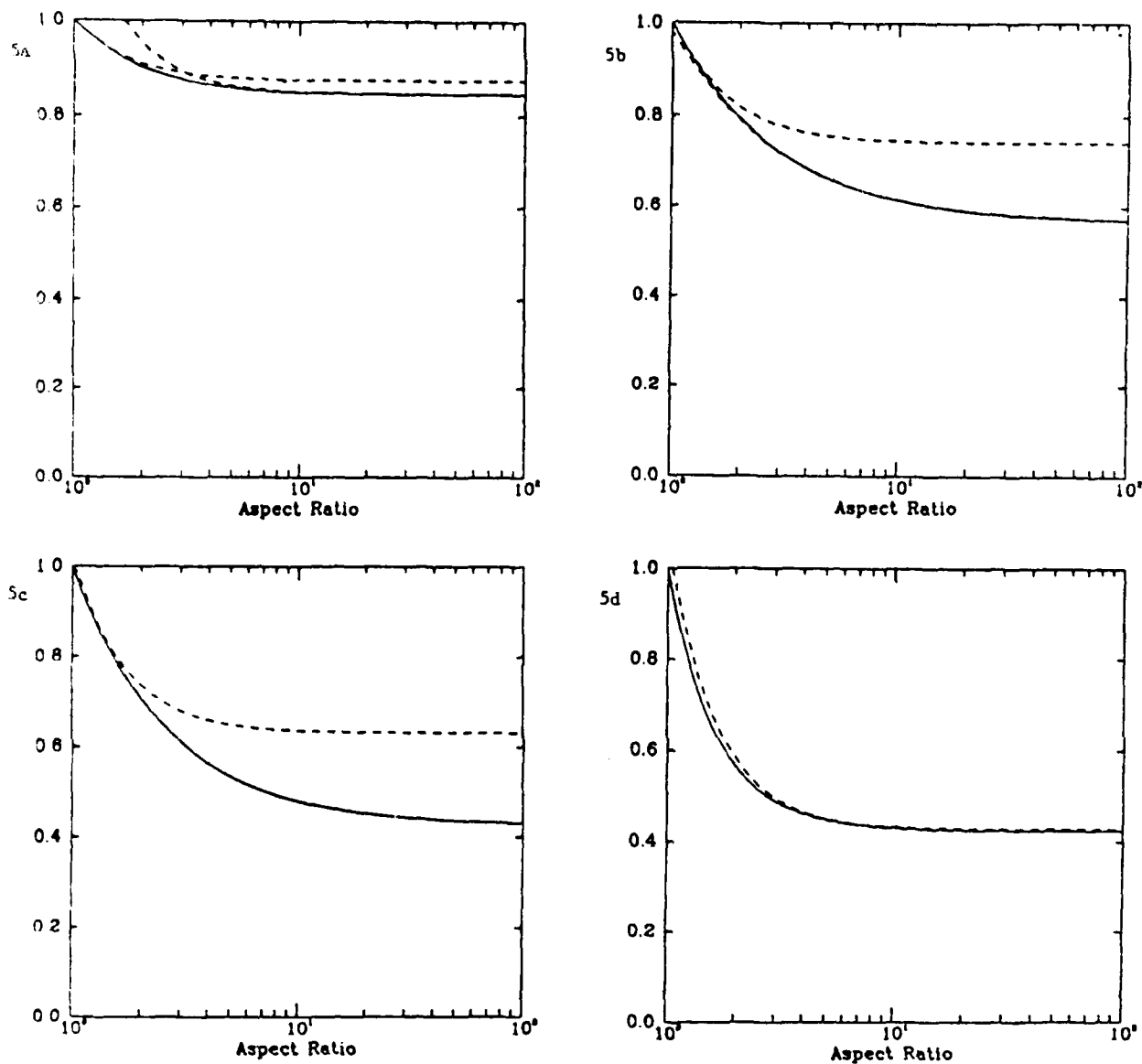


Figure 5. The resistance functions for prolate spheroids, scaled by the results for spheres. The dashed curves are the asymptotic forms of Table 3.

- a. Force/translation (parallel to axis) function X^A .
- b. Force/translation (perpendicular to axis) function Y^A .
- c. Torque/rotation (parallel to axis) function X^C .
- d. Torque/rotation (perpendicular to axis) function Y^C .

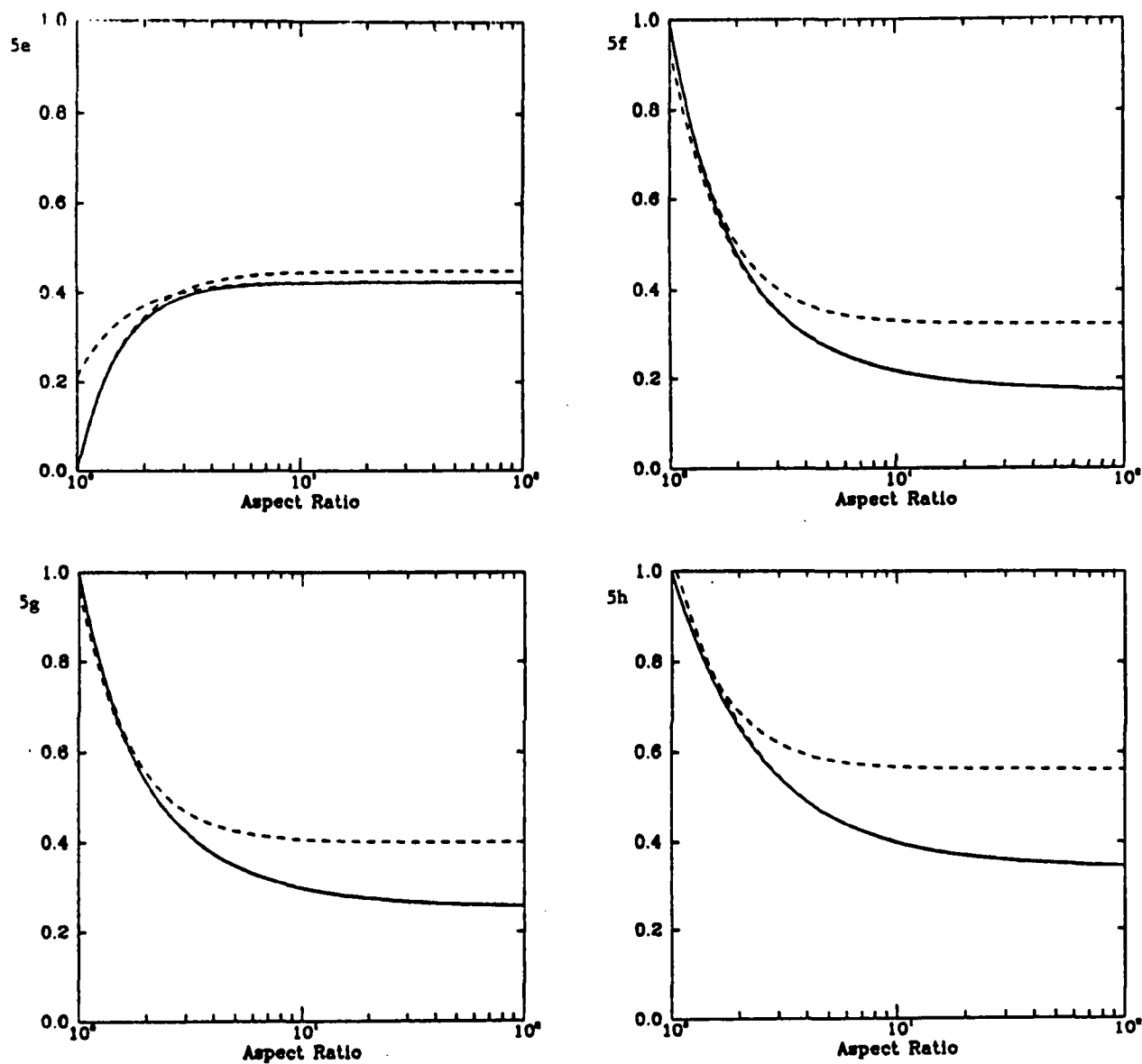


Figure 5. (Continued)

- e. Torque/rate-of-strain function Y^H .
- f. Stresslet/rate-of-strain (axisymmetric straining) function X^M .
- g. Stresslet/rate-of-strain (hyperbolic straining) function Y^M .
- h. Stresslet/rate-of-strain (hyperbolic straining) function Z^M .

so that \underline{C} becomes isotropic and

$$H_{mij}(C^{-1})_{mn}H_{nk\ell} \quad \text{reduces to} \quad 4\pi a^3 Y_d^{(2)}{}_{ijkl}$$

in (3.9), the Faxen law for the stresslet on a torque-free spheroid.

REPORT DOCUMENTATION PAGE		READ INSTRUCTIONS BEFORE COMPLETING FORM
1. REPORT NUMBER 2790	2. GOVT ACCESSION NO. AD-A153503	3. RECIPIENT'S CATALOG NUMBER
4. TITLE (and Subtitle) SINGULARITY SOLUTIONS FOR ELLIPSOIDS IN LOW-REYNOLDS-NUMBER FLOWS: WITH APPLICATIONS TO THE CALCULATION OF HYDRODYNAMIC INTERACTIONS IN SUSPENSIONS OF ELLIPSOIDS	5. TYPE OF REPORT & PERIOD COVERED Summary Report - no specific reporting period	
	6. PERFORMING ORG. REPORT NUMBER	
7. AUTHOR(s) Sangtae Kim	8. CONTRACT OR GRANT NUMBER(s) CPE-8404451 DAAG29-80-C-0041 DMS-8210950, Mod. 1	
9. PERFORMING ORGANIZATION NAME AND ADDRESS Mathematics Research Center, University of 610 Walnut Street Madison, Wisconsin 53706	10. PROGRAM ELEMENT, PROJECT, TASK AREA & WORK UNIT NUMBERS Work Unit Number 2 - Physical Mathematics	
11. CONTROLLING OFFICE NAME AND ADDRESS (See Item 18 below)	12. REPORT DATE February 1985	
	13. NUMBER OF PAGES 36	
14. MONITORING AGENCY NAME & ADDRESS (if different from Controlling Office)	15. SECURITY CLASS. (of this report) UNCLASSIFIED	
	15a. DECLASSIFICATION/DOWNGRADING SCHEDULE	
16. DISTRIBUTION STATEMENT (of this Report) Approved for public release; distribution unlimited.		
17. DISTRIBUTION STATEMENT (of the abstract entered in Block 20, if different from Report)		
18. SUPPLEMENTARY NOTES U. S. Army Research Office P. O. Box 12211 Research Triangle Park North Carolina 27709 National Science Foundation Washington, DC 20550		
19. KEY WORDS (Continue on reverse side if necessary and identify by block number) Sedimentation, Spheroids, Ellipsoids, Low-Reynolds-Number, Hydrodynamic Interaction		
20. ABSTRACT (Continue on reverse side if necessary and identify by block number) The disturbance velocity fields due to translational and rotational motions of an ellipsoid in a uniform stream, constant vorticity and constant rate-of-strain, required in fundamental studies of behavior of suspensions, have been obtained by the singularity method. These solutions extend earlier solutions for prolate spheroids. Although equivalent solutions were obtained by (cont.)		

ABSTRACT (cont.)

Oberbeck (1876), Edwardes (1982) and Jeffery (1922) by separation of variable in ellipsoidal coordinates, the singularity solutions are far more simple in form. Other significant results obtained by the singularity method include the exposition of the unified structure shared by the three boundary value problems and the construction of new forms of the Faxen laws for ellipsoids through application of the reciprocal theorem. The disturbance solutions and Faxen laws, the basis for Smoluchowski's (1911) method-of-reflections technique, are used to calculate hydrodynamic interactions between two or more arbitrarily oriented ellipsoids. In particular, mobility problems are solved directly to order R^{-5} , where R is the centroid-to-centroid separation between the ellipsoids.

END

FILMED

6-85

DTIC